Quasiparticle phonon model description of low-energy states in ^{152}Pr

P. Alexa,[1,*] M. Ramdhane,[2] G. Thiamova,[2] G. S. Simpson,[2] H. R. Faust,[3] J. Genevey,[2] U. Köster,[3] T. Materna,[3,†] R. Orlandi,[4,‡] J. A. Pinston,[2] A. Scherillo,[5] and Z. Hons[6]

[1]*Department of Physics and Institute of Clean Technologies, VŠB—Technical University Ostrava, 17 listopadu 15, CZ-708 33 Ostrava, Czech Republic*

[2]*Université Grenoble Alpes, CNRS, LPSC, Institut Polytechnique de Grenoble, IN2P3, F-38026 Grenoble, France*

[3]*Institut Laue-Langevin, B.P. 156, F-38042 Grenoble Cedex 9, France*

[4]*INFN, Laboratori Nazionali di Legnaro, I-35020 Legnaro, Italy*

[5]*Rutherford Appleton Laboratory, Chilton, Didcot OX11 0QX, United Kingdom*

[6]*Joint Institute for Nuclear Research, Moscow Region, RU-141980 Dubna, Russian Federation and Nuclear Physics Institute, CZ-250 68 Řež, Czech Republic*

(Received 30 June 2017; published 28 March 2018)

Delayed γ-ray and conversion-electron spectroscopy is performed on $A = 152$ fission fragments, at the Lohengrin spectrometer of the Institut Laue-Langevin, providing a new decay scheme for ^{152}Pr. The quasiparticle phonon model, combined with the particle-rotor model, which allows octupole correlations and Coriolis mixing to be taken into account, is applied to analyze its low-energy structure. The main configurations are found to be $(\pi 3/2[422] \otimes \nu 5/2[642])1^+$ for the isomer and $(\pi 3/2[541] \otimes \nu 3/2[521])3^+$ for the ground state.

DOI: 10.1103/PhysRevC.97.034327

I. INTRODUCTION

Nuclei of the neutron-rich $A \sim 150$ region possess numerous interesting features including a rapid spherical-to-prolate ground-state shape change across $N = 88-90$ [1], strong octupole correlations [2,3], rotational bands with identical moments of inertia [4], and isomeric states spanning a wide range of lifetimes [5–9]. Octupole correlations in atomic nuclei are a manifestation of broken reflection symmetry in the nuclear mean field. These modes can be both static and dynamic in nature and arise from the coupling of $\Delta I = \Delta l = 3$ orbits lying close to the Fermi surface. The strongest octupole correlations in the $A \sim 150$ region are predicted around ^{144}Ba [3,10], where the $\pi d_{5/2}$, $h_{11/2}$ and $\nu f_{7/2}$, $\nu i_{13/2}$ orbits lie close to the Fermi surface. Recently a $B(E3; 0^+ \to 3^-)$ value measured by Coulomb excitation for ^{144}Ba showed that octupole collectivity here is larger than any current theoretical prediction [11].

The observation of fast $E1$ transitions between nearly degenerate parity-doublet bands in odd-A nuclei has often been used as an empirical signature of octupole correlations. However, several factors can influence $E1$ decay rates, including shell-correction effects [12], Coriolis mixing, and hexadecapole deformation [13–15]. For example, low $B(E1)$ transition rates between members of parity-doublet bands in ^{146}Ba were determined and have been shown to be due to a cancellation of the intrinsic dipole moments originating from macroscopic and shell-correction effects. However, a $B(E3; 0^+ \to 3^-)$ value was very recently measured for the nucleus ^{146}Ba, which is as large as the one in ^{144}Ba [16].

Strong quadrupole deformation develops in the $A \sim 150$ region beyond $N = 90$, allowing opposite-parity Nilsson orbits with $\Delta K = 0$ to couple via the octupole interaction, assuming the $\mu = 0$ part is dominant [17]. In particular, the Y_{30} interaction couples orbitals with $K^{\pm}[Nn_z\Lambda]$ and $K^{\mp}[N \pm 1\, n_z' \Lambda]$ [13]. For a quadrupole deformation of $\epsilon_2 \sim 0.25$ the $\pi d_{5/2} 3/2[411] - \pi h_{11/2} 3/2[541]$ and $\nu h_{9/2} 3/2[521] - \nu i_{13/2} 3/2[651]$ couplings approach the Fermi surface at $Z \sim 60$ and $N \sim 90$. The $\pi 3/2[541]$ orbital has been assigned as the ground state of ^{151,153}Pr [7,18,19], hence octupole correlations may manifest themselves in these nuclei. Indeed the existence of a possible parity doublet band has been proposed in ^{151}Pr [18–20], though a 35.1-keV isomeric state with a 50(8)-μs half-life, decaying by an $E1$ transition, has also been reported in the same nucleus [7]. The neutron-rich Pr nuclei are thus an interesting test ground for models able to calculate $E1$ transition rates.

In the present work we have measured delayed γ rays and conversion electrons from an isomeric state in ^{152}Pr and interpreted the structure of states in delayed cascades using the quasiparticle-phonon model plus the particle-rotor model (QPM + PRM). Pr nuclei are difficult to study from both an experimental and a theoretical point of view. Their complementary partners following the spontaneous fission of ^{248}Cm and ^{252}Cf are the Rb and Y nuclei, which possess both fragmented level schemes and isomeric states, making mass identification via relative γ-ray intensities difficult. This is further complicated by some of the even-even core nuclei possessing rotational ground-state bands with identical moments of inertia [4], resulting in intraband transitions with approximately the same energy in neighboring isotopes. The mass assignments of various rotational bands to $^{151-153}$Pr have changed several times [7,18,19,21], however, a prompt γ-ray

*Corresponding author: petr.alexa@vsb.cz
†Present address: CEA, Saclay, France.
‡Present address: ASRC, JAEA, Tokai, Japan.

spectroscopy experiment, performed in conjunction with the VAMOS spectrometer, permitting firm A and Z identification, has recently improved the experimental situation [20]. The theoretical task of assigning Nilsson orbitals to the various rotational bands can be difficult for Pr nuclei here, as $K = 1/2$ orbitals of both parities and large j values are present near the Fermi surface. Moreover, the positive-parity orbitals are expected to be mixtures of $\pi g_{7/2}$ and $\pi d_{5/2}$ and can have either sign of signature splitting or a near-cancellation for certain admixtures. Studies of isomeric transitions and allowed unhindered β decays, both of which can take place only between nucleons occupying a handful of orbitals, can allow firm configuration assignments to be made.

II. EXPERIMENT

Delayed γ-ray and conversion-electron spectroscopy of $A = 152$ fission fragments was performed at the Lohengrin mass spectrometer of the high-flux reactor at the Institut Laue-Langevin, Grenoble. Neutron-rich $A = 152$ nuclei were produced using an 0.870 mg/cm^2, 7×0.5 cm^2, ^{241}Am target, which mostly fissioned following the capture of two thermal neutrons. The Lohengrin mass spectrometer selected nuclei recoiling from the target, according to their mass–to–ionic charge and kinetic energy–to–ionic charge ratios. The flight time of $A = 152$ nuclei through the spectrometer was around 3.1 μs, allowing decays from microsecond isomers to be observed at the focal point. The kinetic energies, and hence masses, of the fission fragments were identified by a split-anode $\Delta E1$-$\Delta E2$ ionization chamber. Two experimental setups were used in this measurement. In the first, two Clover Ge detectors were placed in a compact geometry perpendicular to the beam for γ-ray spectroscopy studies. In the second, a twofold segmented liquid-nitrogen-cooled Si(Li) conversion-electron detector was included in the setup. Each segment had areas of 3×2 cm^2 and a total efficiency of ∼15%. This detector was placed behind a 6-μm-thick Mylar foil, situated at the end of the ionization chamber. The gas pressure in the chamber was tuned to stop the ions in the last 1 μm of the Mylar foil. Any γ rays or electrons detected up to 40 μs after the arrival of an ion were recorded on disk for off-line analysis. The experiment was performed during the same campaign as the work reported in Refs. [6,7], and more details on the setup can be found therein.

III. EXPERIMENTAL RESULTS

Background-subtracted delayed γ rays detected up to 10 μs after the arrival of an $A = 152$ ion are shown in Fig. 1. Here the background was taken from a cut towards the end of the 40-μs time window. Delayed transitions with energies of 115.1(3) and 98.1(3) keV are visible, along with Pr x rays. These results partially agree with previous β-decay studies of ^{152}Pr where a delayed 114.8(2)-keV γ ray was reported [22,23]. However, in those works a 97.7(2)-keV transition was reported to be prompt. Similarly, a weak 98.1-keV transition was reported to be prompt in the fission spectroscopy data in [20].

Background-subtracted delayed conversion electrons and photons measured in the Si(Li) detectors are shown in Fig. 2. Here K and L conversion-electron peaks from the 115.1-keV transition can clearly be seen, along with weaker ones from the 98.1-keV decay and Pr x rays. Additionally, a γ ray with an energy of 17.0(4) keV is also visible.

The sum of the 17.0- and 98.1-keV γ-ray energies equals that of the 115.1-keV transition and these are likely parallel decay branches from the same isomer. The 98.1- and 115.1-keV transitions were measured to have the same half-lives, within errors, giving additional evidence that they originate from the same isomeric state.

From the γ-ray and electron-peak areas conversion coefficients of $\alpha_K = 0.93(12)$, $\alpha_L = 0.32(11)$, and $\alpha_K/\alpha_L = 2.8(10)$ were obtained for the 115.1-keV transition. These results are in good agreement with the theoretical values for an $E2$ decay, which are 0.801(12), 0.380(6), and 2.110(48), respectively [24]. When these three numbers are considered together the 115.1-keV transition can be uniquely assigned as $E2$ in nature.

The relative intensities of delayed γ rays measured using the Ge and Si(Li) detectors are listed in Table I. As the 17.0-

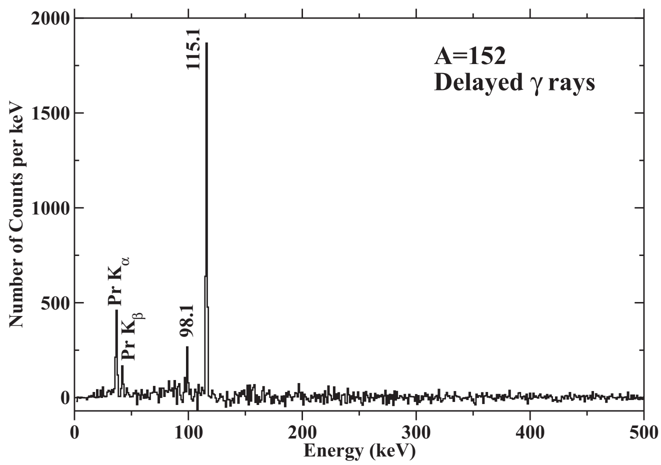

FIG. 1. Delayed γ rays observed in the Ge detectors in coincidence with $A = 152$ ions.

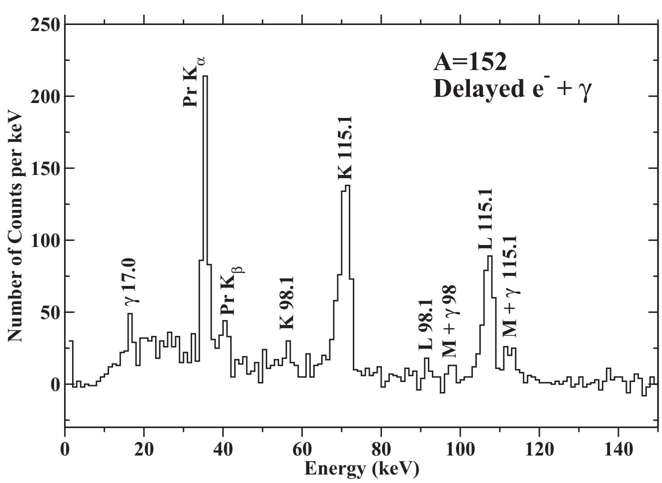

FIG. 2. Delayed conversion electrons and photons observed in the Si(Li) detector in delayed coincidence with $A = 152$ ions.

TABLE I. Level energies, delayed γ-ray energies, and intensities and total intensities of the delayed cascade from the 115.1-keV isomeric state.

E_{level} (keV)	E_γ (keV)	EL	I_γ (rel.)	I_{Total} (rel.)
98.1	98.1	$E1$	18(3)	23(3)[b]
115.1	17.0	$E1$	2.3(11)	15(8)[b]
	115.1	$E2$	100(5)[a]	228(12)[b]

[a]Reference transition ($I_\gamma = 100$).
[b]Calculated using theoretical conversion coefficients [24].

and 98.1-keV γ rays are in cascade, and parallel to the 115.1-keV $E2$ transition, when corrected for internal conversion ($\alpha_{17.0} = 5.66$, $\alpha_{98.1} = 0.265$ [24]), consistent total intensities are obtained only when the 17.0- and 98.1-keV transitions both have $E1$ multipolarities.

The half-life of the isomer was obtained by fitting an exponential function to the time distribution of 115.1-keV γ rays, relative to the arrival of an $A = 152$ ion. This is shown in Fig. 3 and $T_{1/2} = 4.7(3)\mu$s was determined. The $T_{1/2}$ measured in the present experiment is close to $T_{1/2} = 4.1(1)$ μs, previously reported in β-decay studies [23], though incompatible with the earlier value of $T_{1/2} = 1.0(3)$ μs [22].

Combining all the above information allowed the partial level scheme shown in Fig. 4 to be created. The order of the 17.0- and 98.1-keV transitions was determined assuming that the latter decay is the same as that of the 97.7-keV γ ray reported as prompt in β-decay studies [22,23]. The spin assignments are made using the results of the theoretical calculations described in Sec. V.

IV. QUASIPARTICLE PHONON MODEL

In the QPM + PRM for odd-odd nuclei the total Hamiltonian is written as

$$H = H_{\text{int}} + H_{\text{rot}} \tag{1}$$

where H_{int} is the intrinsic Hamiltonian and H_{rot} is the rotational Hamiltonian [25], which contains the Coriolis interaction

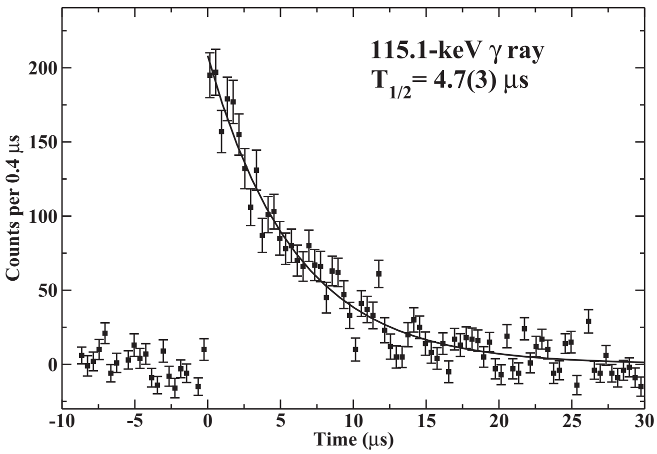

FIG. 3. Time spectrum of 115.1-keV γ rays detected in the Ge detectors, relative to the arrival of an $A = 152$ ion.

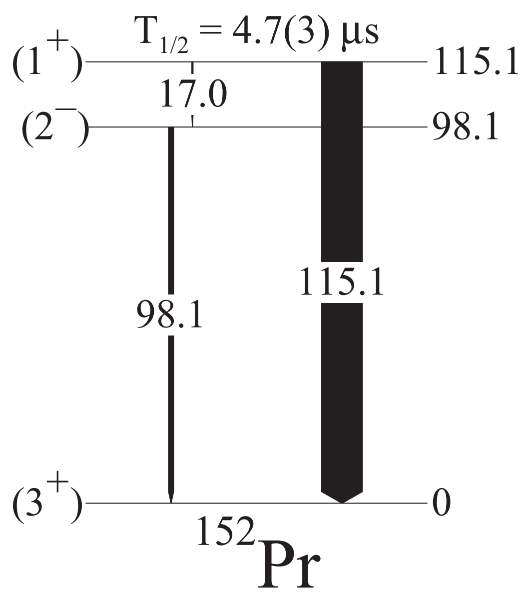

FIG. 4. Partial level scheme of ^{152}Pr obtained in this work.

responsible for the coupling of intrinsic and rotational degrees of freedom,

$$\begin{aligned} H_{\text{rot}} &= \sum_{i=1,2} \frac{\hbar^2}{2J}(\hat{I}_i - \hat{j}_i)^2 \\ &= \frac{\hbar^2}{2J}\left(\hat{I}_i^2 - \hat{I}_3^2\right) + \frac{\hbar^2}{4J}\chi_{\text{rec}}(\hat{j}_+\hat{j}_- + \hat{j}_-\hat{j}_+) \\ &\quad - \frac{\hbar^2}{2J}\chi_{\text{cor}}(\hat{I}_+\hat{j}_- + \hat{I}_-\hat{j}_+), \end{aligned} \tag{2}$$

where J is the moment of inertia with respect to the rotation axis and $\hat{I}_i$ and $\hat{j}_i$ are components of the total and intrinsic angular momentum, respectively. The second term on the right-hand side is the recoil term, the last term represents the Coriolis interaction, and χ_{rec} and χ_{cor} are the recoil and Coriolis attenuation factors, respectively.

The intrinsic Hamiltonian can be written as [26]

$$H_{\text{int}} = H_{\text{AV}} + H_{\text{Pair}} + H_{\text{Mult}} + H_{\text{np}}, \tag{3}$$

where H_{AV} is the axially symmetric quadrupole and hexadecapole deformed average mean field (Nilsson),

$$H_{\text{Pair}} = -\Sigma_{\tau=p,n} G_\tau P_\tau^+ P_\tau \tag{4}$$

is the short-range monopole pairing interaction, and

$$H_{\text{Mult}} = -\tfrac{1}{2}\Sigma_{\tau=p,n}\Sigma_{\lambda,\mu}\kappa_{\lambda,\mu}^{\tau} Q_{\lambda,\mu}^{\tau+}(\hat{r}) Q_{\lambda,\mu}^{\tau}(\hat{r}) \tag{5}$$

represents the long-range separable quadrupole-quadrupole ($\lambda = 2$) and octupole-octupole interaction ($\lambda = 3$). The multipole-multipole interaction strengths $\kappa_{\lambda,\mu}^{p} = \kappa_{\lambda,\mu}^{n}$ and are fitted to experimental phonon energies of the even-even core or taken from the systematics. All terms in the two-qp neutron-proton interaction in H_{Mult} are replaced with a diagonal δ force H_{np} with central and spin-spin components, i.e., $H_{\text{np}} = \delta(\vec{r}_p - \vec{r}_n)(u_0 + u_1\vec{\sigma}_p\vec{\sigma}_p)$, where the parameters u_0 and u_1 can be taken from the systematics of the Gallagher-Moszkowski

TABLE II. Possible Nilsson configurations of the ground, 98.1-keV, and 115.1-keV states of ^{152}Pr. The notation used for the Nilsson orbitals is $K[Nn_z\Lambda]$. The spin and parity J^π are listed to the right of each Nilsson configuration.

Ground state	98.1-keV state	115.1-keV state
$(\pi\frac{3}{2}[541]\otimes\nu\frac{5}{2}[642])4^-$	$(\pi\frac{3}{2}[541]\otimes\nu\frac{3}{2}[521])3^+$	$(\pi\frac{1}{2}[420]\otimes\nu\frac{3}{2}[521])2^-$
$(\pi\frac{3}{2}[541]\otimes\nu\frac{3}{2}[521])3^+$	$(\pi\frac{1}{2}[420]\otimes\nu\frac{3}{2}[521])2^-$	$(\pi\frac{3}{2}[422]\otimes\nu\frac{5}{2}[642])1^+$
$(\pi\frac{3}{2}[422]\otimes\nu\frac{3}{2}[521])0^-$	$(\pi\frac{3}{2}[422]\otimes\nu\frac{5}{2}[642])1^+$	$(\pi\frac{1}{2}[420]\otimes\nu\frac{3}{2}[521])2^-$
$(\pi\frac{3}{2}[422]\otimes\nu\frac{5}{2}[642])1^+$	$(\pi\frac{1}{2}[420]\otimes\nu\frac{3}{2}[521])2^-$	$(\pi\frac{3}{2}[541]\otimes\nu\frac{3}{2}[521])3^+$

(GM) [27] splitting and Newby shifts [28] for rare-earth nuclei [29].

In the QPM first the BCS transformation from nucleon to quasiparticle operators is performed and then phonon operators are constructed as linear superpositions of pairs of qp operators. The phonon energies and wave functions are obtained by solving the standard RPA equations. Taking into account the coupling between the odd nucleons and the vibrating even-even core results in the intrinsic wave functions

$$|\psi_\varrho(K^\pi)\rangle = \left(\sum_{\nu_n\nu_p} C^{K\varrho}_{\nu_n\nu_p}\alpha^\dagger_{\nu_n}\alpha^\dagger_{\nu_p} + \sum_{\nu_n\nu_p\lambda\mu} D^{K\varrho}_{\lambda\mu\nu_n\nu_p}\alpha^\dagger_{\nu_n}\alpha^\dagger_{\nu_p}Q^\dagger_{\lambda\mu}\right)|\rangle, \qquad (6)$$

where the amplitudes $C^{K\varrho}_{\nu_n\nu_p}$ of neutron-proton two-qp components, $\alpha^\dagger_{\nu_n}\alpha^\dagger_{\nu_p}|\rangle$, and the amplitudes $D^{K\varrho}_{\lambda\mu\nu_n\nu_p}$ of two-qp plus phonon components, $\alpha^\dagger_{\nu_n}\alpha^\dagger_{\nu_p}Q^\dagger_{\lambda\mu}|\rangle$, in the odd-odd nucleus intrinsic wave function $|\psi_\varrho(K^\pi)\rangle$ are determined using the variational principle.

In the last step the matrix of the total Hamiltonian $H = H_{\rm int} + H_{\rm rot}$ is constructed and diagonalized in the basis of the symmetrized wave functions $|IMK\rho\rangle$ in the laboratory system, where ρ characterizes the intrinsic states. A more detailed description of the method can be found in Ref. [26].

The parameters of the Nilsson potential we use in our calculations are those recommended in Soloviev's monograph [30]. Initial values of the quadrupole and hexadecapole deformation parameters and of the ground-state pairing gaps are taken from finite-range droplet model plus shell correction (FRDM) calculations [10] and the neutron-proton interaction parameters are fixed to be $u_0 = -4.03$ MeV and $u_1 = -0.89$ MeV.

V. CALCULATION RESULTS

The 115.1-keV isomeric state of ^{152}Pr decays either by a delayed $E2$ transition to the ground state or by a 17.0-keV, $E1$ transition to the 98.1-keV level, which then decays by another $E1$ transition to the ground state. This decay sequence enables the relative parities of the three levels in question to be established.

To obtain reliable Nilsson assignments for low-lying states in ^{152}Pr one has to rely on the Nilsson assignments in the neighboring odd-A nuclei ^{151}Pr and ^{151}Ce. Assuming the proton and neutron Nilsson orbitals close to the Fermi level to be $\pi 3/2[422]$, $\pi 3/2[541]$, and $\pi 1/2[420]$ and $\nu 3/2[521]$, $\nu 5/2[642]$ [6,15], respectively, enables four possible scenarios for the spins of the three levels to be determined, imposing that the ground state should correspond to the spin-triplet member of the corresponding GM doublet (Table II).

Note also that the GM spin-singlet partners of the proposed ground-state configurations cannot be considered to correspond to one of the two excited states because they differ by $\Delta I = 3$ with respect to the spin-triplet case and thus would not decay preferentially by either an $E1$ or an $E2$ transition.

Among those four scenarios, the last two do not seem to correspond to any recent experimental data and only the first two are tested in detail.

As the $\nu 5/2[642]$ and $\nu 3/2[521]$ neutron orbitals are ~200 keV apart in ^{151}Ce and ^{153}Nd [6], both are candidates for the lowest neutron orbital in ^{152}Pr and we suppose that the ground-state configuration of ^{152}Pr is either $\pi 3/2[541]\otimes\nu 5/2[642]$ or $\pi 3/2[541]\otimes\nu 3/2[521]$. Based on the GM coupling rules [27], these two configurations give $K^\pi = 4^-$ and $K^\pi = 3^+$, respectively, for the bandhead. Note that high-spin states in the favored signature sequence are easier to populate in an odd-odd nucleus.

To determine with confidence the parity of the ground state of ^{152}Pr it is helpful to know the spin and parity of the 1827.5-keV level in ^{152}Nd, to which the ground-state decay of ^{152}Pr strongly feeds, with the lowest $\log ft$ value in the decay scheme, 4.9 [31,32]. This $\log ft$ is characteristic of an unhindered allowed β decay [33], and even here open questions exist. Hellström *et al.* [31,34] assigned the spin and parity of the 1827.5-keV level to be 3^- based on the calculated K conversion coefficient 0.040(15) for the 285.0-keV transition to the 2^- level at 1542.0 keV, thus indicating its multipolarity to be $M1$ or $E2$. It should be noted that the conversion coefficient was calculated indirectly from the coincident intensities of γ and x rays. Toh *et al.* [32] assigned the spin and parity of the 1827.5-keV level to be 3^+, based on direct γ and conversion-electron measurements that gave $\alpha_K = 0.014(3)$ for the 285-keV transition, compatible with an $E1$ multipolarity.

The value of the $\log ft = 4.9$ also indicates a large overlap of the initial and the final wave functions, which suggests that the 1827.5-keV level should probably have a large component of a simple, two-qp excitation. We have tested the hypothesis of Hellstrom *et al.* that the 1827.5-keV level is an octupole $K = 3^-$ bandhead within the framework of the QPM for the even-even nucleus ^{152}Nd. Proton and neutron pairing gaps of 0.869 and 0.709 MeV, respectively, Coriolis and recoil attenuation parameters of 0.85 and 0.6, respectively, and the

TABLE III. Structure of the two lowest 3^- bandheads in ^{152}Nd. The first two rows of data are calculations with $\epsilon_2 = 0.24$ and the shift of the $i_{13/2}$ neutron subshell at -2 MeV. The two rows in the middle correspond to a calculation with $\epsilon_2 = 0.29$ and the shift of the $i_{13/2}$ neutron subshell at -1 MeV. The last two rows of data were obtained with parameters $\epsilon_2 = 0.29$ and the shift of the $i_{13/2}$ neutron subshell at -2 MeV. The last column lists the total contributions of all two-quasineutron components, one of which is $\frac{5}{2}$[642].

	$E_{\rm exc}$ (MeV)	$\nu\frac{3}{2}[651] \otimes \nu\frac{3}{2}[521]$ (%)	$\nu\frac{3}{2}[651] \otimes \nu\frac{3}{2}[531]$ (%)	$\nu\frac{5}{2}[642]$ (%)
3^-_1	1.5	25	15	5
3^-_2	1.8	73	12	1.5
3^-_1	1.2	42	2	0.7
3^-_2	1.5	57	2	0.5
3^-_1	1.5	29	3	12
3^-_2	1.6	16	0.04	83

same phonon energies as in [15] were used. Deformations of $\epsilon_2 = 0.24$ and $\epsilon_4 = -0.07$ were employed in the calculations, taken from recent FRDM calculations [10]. Our calculations show that the lowest 3^- bandhead occurs around 1.3–1.4 MeV and is more collective with a dominant two-qp neutron component $\nu3/2[651] \otimes \nu3/2[521]$ (about 30%) and the components containing the neutron configuration $\nu5/2[642]$ represent only about 3%. The second, less collective, 3^- bandhead occurs at around 1.5–1.6 MeV and has a more pronounced two-qp character (dominant configuration $\nu3/2[651] \otimes \nu3/2[521]$, about 70%). Here the neutron orbital $\nu5/2[642]$ is present with a probability of about 1%. If we run the calculations for a higher value of $\epsilon_2 \sim 0.29$, corresponding to the value derived from the experimental $B(E2; 0^+_1 \rightarrow 2^+_1) = 159 \pm 10$ W.u. (Weisskopf units) [35], the energy of the lowest 3^- bandhead remains more or less unchanged. It is less collective, has the same dominant configuration, and components containing the $\nu5/2[642]$ orbital represent about 12% of the wave function. In fact the $\nu11/2[505] \otimes \nu5/2[642]$ component is the strongest one in this state (9%) but it cannot give rise to an allowed transition. The structure of the second 3^- bandhead is more sensitive to the shift of the $i_{13/2}$ neutron subshell. For lower values of the shift (-2 MeV), the $\nu11/2[505] \otimes \nu5/2[642]$ configuration becomes dominant (about 80%) and other configurations containing the $\nu5/2[642]$ orbital are smaller than 1%. However, the $\nu11/2[505] \otimes \nu5/2[642]$ configuration does not permit an allowed β-decay transition if the ground-state configuration of ^{152}Pr is $4^-(\pi3/2[541] \otimes \nu5/2[642])$. The situation is summarized in Table III.

To shift the energy of the lowest 3^- state to the experimental energy of 1827.5 keV, proton and neutron pairing gaps larger than 1 MeV would be necessary. However, in this case the lowest 3^- state would become more collective, with individual neutron and proton two-qp components smaller than 10%, and components containing $\nu5/2[642]$ would represent only about 3% for both quadrupole deformations tested ($\epsilon_2 = 0.24$ and 0.29). As a consequence, the β-decay transition from the $4^-(\pi3/2[541] \otimes \nu5/2[642])$ ground state of ^{152}Pr to the 3^-

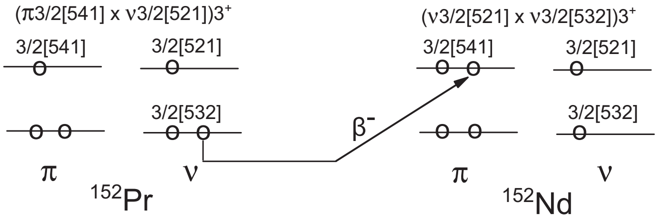

FIG. 5. Schematic of the proposed β decay of the ground state of ^{152}Pr to a $(\nu3/2[521] \otimes \nu3/2[532])3^+$ two-quasiparticle state in ^{152}Nd.

state in ^{152}Nd could not be characterized by such a low log ft value.

On the other hand, a natural interpretation of the β decay of ^{152}Pr into ^{152}Nd may be proposed by assuming the ground state of ^{152}Pr to be 3^+. Let us assume an allowed transition from a 3^+ ground state in ^{152}Pr, with a configuration $\pi3/2[541] \otimes \nu3/2[521]$, to a 3^+ state in ^{152}Nd. Using $\epsilon_2 = 0.24$, and neglecting interactions between the quasiparticles, in our calculations two 3^+ states close in energy to 1.8 MeV are present, namely, $\nu5/2[642] \otimes \nu1/2[660]$ at 1.9 MeV and $\nu3/2[521] \otimes \nu3/2[532]$ at 2.0 MeV. A β decay to the latter configuration would satisfy all the selection rules for allowed transitions, because $\Delta N = 0, \Delta n_z + \Delta\Lambda = 0$ and $|\Delta n_z| \leqslant 2$. More precisely, the coupled-nucleon transformation mechanism for β decay suggested in [33] can be applied. Here the transforming neutron in ^{152}Pr occupies the $\nu3/2[532]$ orbital, located just below the $\nu3/2[521]$ orbital of the unpaired neutron, and transforms into a proton occupying the $\pi3/2[541]$ orbital in the even-even core, with the $\nu3/2[521] \otimes \nu3/2[532]$ two-qp state strongly fed. This is illustrated schematically in Fig. 5. A ^{152}Pr ground-state configuration of $\pi3/2[541] \otimes \nu3/2[521]$ is also in agreement with the global microscopic calculations of ground-state spins and parities in Ref. [36], giving $K^\pi_p = 3/2^-, K^\pi_n = 3/2^-$.

The ground state 3^+ $\pi3/2[541] \otimes \nu3/2[521]$ configuration assignment is supported by the analysis of experimental electromagnetic transitions between low-lying states in ^{152}Pr. One observes that for cases 1 and 4 in Table II an $E2$ transition from the isomer would be forbidden to a first-order approximation, because both the proton and the neutron orbitals change. On the other hand, an $E1$ transition from the 115.1-keV, (2^-) to the 98.1-keV (3^+) state would be, to first order, allowed because only the proton configuration changes in both cases. These scenarios do not correspond to the measured $E1$ transition branching ratio and the reduced transition rate of $B(E1) = 9.6(5) \times 10^{-8}$ W.u. deduced from the experimental half-life. Our QPM calculations predict $B(E1; 2^- \rightarrow 3^+) = 1.0 \times 10^{-4}$ W.u. For case 3 in Table II the $E2$ transition from the 115.1-keV (2^-) level to the 0-keV (0^-) state is, to first order, allowed and is incompatible with the $B(E2) = 0.049(4)$ W.u. derived from the measured isomer half-life and 115.1-keV γ-ray intensity. In case 2 both the $E2$ and the $E1$ transitions from the 1^+ state are forbidden, to first order, because both the proton and the neutron orbitals change. This scenario seems to correspond best to a microsecond lifetime for the 115-keV state.

VI. CONCLUSION

The decay of a 115.1-keV, 4.7(3)-μs isomeric state of ^{152}Pr has been measured via delayed γ-ray and conversion-electron spectroscopy. This has allowed multipolarities of $E1$ and $E2$ to be assigned to the 17.0- and 115.1-keV transitions out of the isomer, respectively, with reduced transition rates of $B(E1) = 9.6(5) \times 10^{-8}$ and $B(E2) = 0.049(4)$ W.u. The decay of the 98.1-keV transition was determined to be $E1$ in nature. A comparison with existing β-decay data and the results of QPM calculations have allowed the ground-state configuration and spin of $(\pi 3/2[541] \otimes \nu 3/2[521])3^+$ to be assigned. A similar comparison between the experimental data and the QPM calculations assigned the isomeric state as $(\pi 3/2[422] \otimes \nu 5/2[642])1^+$ and the 98.1-keV level as $(\pi 1/2[420] \otimes \nu 3/2[521])2^-$.

ACKNOWLEDGMENTS

This work was supported by the National Programme for Sustainability I (2013–2020) financed by the state budget of the Czech Republic, identification code LO1406. G.T. acknowledges the financial support of the Congé Pour Recherches et Conversions Thématiques (CRCT), the Czech Academy of Sciences and the French-Czech LEA NuAG collaboration.

[1] R. F. Casten, Phys. Rev. C **33**, 1819 (1986).
[2] W. R. Phillips, I. Ahmad, H. Emling, R. Holzmann, R. V. F. Janssens, T. L. Khoo, and M. W. Drigert, Phys. Rev. Lett. **57**, 3257 (1986).
[3] G. Leander, W. Nazarewicz, P. Olanders, I. Ragnarsson, and J. Dudek, Phys. Lett. B **152**, 284 (1985).
[4] S. J. Zhu *et al.*, J. Phys. G: Nucl. Part. Phys. **21**, L57 (1995).
[5] T. Rzaca-Urban, W. Urban, J. A. Pinston, G. S. Simpson, A. G. Smith, J. F. Smith, and I. Ahmad, Phys. Rev. C **82**, 067304 (2010).
[6] G. S. Simpson, W. Urban, J. A. Pinston *et al.*, Phys. Rev. C **81**, 024313 (2010).
[7] T. Malkiewicz, G. S. Simpson, W. Urban *et al.*, Phys. Rev. C **85**, 044314 (2012).
[8] P. C. Sood, M. Sainath, R. Gowrishankar, and K. V. Sai, Phys. Rev. C **83**, 027303 (2011).
[9] P. C. Sood, R. Gowrishankar, and K. V. Sai, J. Phys. G **39**, 095107 (2012).
[10] P. Möller, A. Sierk, T. Ichikawa, and H. Sagawa, At. Dat. Nucl. Dat. Tables **109**, 1 (2016).
[11] B. Bucher, S. Zhu, C. Y. Wu *et al.*, Phys. Rev. Lett. **116**, 112503 (2016).
[12] P. Butler and W. Nazarewicz, Nucl. Phys. A **533**, 249 (1991).
[13] P. A. Butler and W. Nazarewicz, Rev. Mod. Phys. **68**, 349 (1996).
[14] D. Nosek, R. K. Sheline, P. C. Sood, and J. Kvasil, Z. Phys. A **344**, 277 (1992).
[15] G. Thiamova, P. Alexa, Z. Hons, and G. S. Simpson, Phys. Rev. C **86**, 044334 (2012).
[16] B. Bucher, S. Zhu, C. Y. Wu *et al.*, Phys. Rev. Lett. **118**, 152504 (2017).
[17] W. Nazarewicz and S. L. Tabor, Phys. Rev. C **45**, 2226 (1992).
[18] J. K. Hwang, A. V. Ramayya, J. H. Hamilton, S. H. Liu, N. T. Brewer, Y. X. Luo, J. O. Rasmussen, S. J. Zhu, and R. Donangelo, Phys. Rev. C **82**, 034308 (2010).
[19] J. K. Hwang, A. V. Ramayya, J. H. Hamilton, S. H. Liu, N. T. Brewer, Y. X. Luo, J. O. Rasmussen, S. J. Zhu, and R. Donangelo, Phys. Rev. C **82**, 049901(E) (2010).
[20] E. H. Wang, A. Lemasson, J. H. Hamilton *et al.*, Phys. Rev. C **92**, 034317 (2015).
[21] J. K. Hwang, A. Lemasson, J. H. Hamilton *et al.*, Phys. Rev. C **62**, 044303 (2000).
[22] I. Tago, Y. Kawase, and K. Okano, Z. Phys. A **335**, 477 (1990).
[23] S. Yamada, A. Taniguchi, and K. Okano, J. Phys. Soc. Jpn. **64**, 4047 (1995).
[24] T. Kibédi *et al.*, Nucl. Instrum. Meth. Phys. Res. A **589**, 202 (2008).
[25] P. Alexa, Z. Hons, and J. Kvasil, J. Phys. G **36**, 045103 (2009).
[26] J. Kvasil, R. K. Sheline, V. O. Nesterenko, I. Hřivnáčová, and D. Nosek, Z. Phys. A **343**, 145 (1992).
[27] C. J. Gallagher and S. A. Moszkowski, Phys. Rev. **111**, 1282 (1958).
[28] N. D. Newby, Phys. Rev. **125**, 2063 (1962).
[29] A. K. Jain *et al.*, Rev. Mod. Phys. **70**, 843 (1998).
[30] V. Soloviev, *Theory of Complex Nuclei* (Pergamon Press, Oxford, UK 1976).
[31] M. Hellström, B. Fogelberg, H. Mach, D. Jerrestam, and L. Spanier, Phys. Rev. C **46**, 860 (1992).
[32] Y. Toh, S. Yamada, A. Taniguchi, and Y. Kawase, Eur. Phys. J. A **2**, 331 (1998).
[33] P. C. Sood and R. K. Sheline, At. Dat. Nucl. Dat. Tables **43**, 259 (1989).
[34] M. Hellström, H. Mach, B. Fogelberg, D. Jerrestam, and L. Spanier, Phys. Rev. C **47**, 545 (1993).
[35] M. Hellström, H. Mach, B. Fogelberg, D. Jerrestam, and L. Spanier, Phys. Rev. C **43**, 1462 (1991).
[36] L. Bonneau, P. Quentin, and P. Möller, Phys. Rev. C **76**, 024320 (2007).